



Published in final edited form as:

*Mol Pharm.* 2013 May 6; 10(5): 1725–1735. doi:10.1021/mp300561y.

## Design of Hybrid Lipid/Retroviral-Like Particle Gene Delivery Vectors

Rahul K. Keswani<sup>1</sup>, Ian M. Pozdol<sup>1</sup>, and Daniel W. Pack<sup>1,2,\*†</sup>

<sup>1</sup> Department of Chemical and Biomolecular Engineering, University of Illinois, Urbana-Champaign, Urbana, IL 61801

<sup>2</sup> Department of Bioengineering, University of Illinois, Urbana-Champaign, Urbana, IL 61801

### Abstract

Recombinant retroviruses provide highly efficient gene delivery and the potential for stable gene expression. The retroviral envelope protein, however, is the source of significant disadvantages such as immunogenicity, poor stability (half-life of transduction activity of 5–7 h at 37 °C for amphotropic murine leukemia virus) and difficult production and purification. To address these problems, we report construction of efficient hybrid vectors through association of murine leukemia virus (MLV)-like particles (M-VLP) with synthetic liposomes comprising DOTAP, DOPE and cholesterol ( $\phi$ /M-VLP). We conclude that the lipid composition is a significant determinant of the transfection efficiency and uptake of  $\phi$ /M-VLP in HEK293 cells with favorable compositions for transfections being those with low DOTAP, low DOPE and high cholesterol content. Cellular uptake, however, was dependent on DOTAP content alone. By extrusion of liposomes prior to vector assembly, the size of these hybrid vectors could also be decreased to  $\approx$ 300 nm, as confirmed via DLS and TEM.  $\phi$ /M-VLP were also robust on storage in terms of vector size and transfection efficiency and provided stable transgene expression over a period of three weeks. We conclude that the non-covalent combination of biocompatible synthetic lipids with inactive retroviral particles to form a highly efficient hybrid vector is a significant extension to the development of novel gene delivery platforms.

### Keywords

Hybrid Gene Delivery Vectors; Murine Leukemia Virus-Like Particles; DOTAP; DOPE; Cholesterol

## INTRODUCTION

Gene therapy can potentially treat inherited diseases<sup>1,2</sup> as well as acquired diseases such as cancers<sup>3</sup>, cardiovascular diseases<sup>1</sup>, intraocular diseases<sup>1</sup> and viral infections<sup>4,5</sup>. However, this revolutionary method has yet to deliver on its promise due in large part to the lack of safe and efficient means of delivering therapeutic genes<sup>6</sup>. Delivery of genes to mammalian cells can be achieved via vectors such as recombinant viruses or synthetic molecules including lipids and polymers<sup>7</sup>.

\*Correspondence should be addressed to D.W.P. Department of Pharmaceutical Sciences University of Kentucky 467 Biological Pharmaceutical Building 789 S. Limestone Lexington, KY 40536-0596, USA Phone: 859-218-0907 dan.pack@uky.edu.

†Current address: Department of Chemical & Materials Engineering and Department of Pharmaceutical Sciences University of Kentucky 467 Biological Pharmaceutical Building 789 S. Limestone Lexington, KY 40536-0596

### CONFLICT OF INTEREST

The authors declare no competing financial interest.

Viruses have evolved to efficiently transfer their own genetic material into cells and have developed highly efficient mechanisms for navigating the barriers to cellular transduction. Retroviruses were the earliest class of viruses used for gene therapy clinical trials because of their relatively simple genomic architecture and capacity to integrate their genetic cargo within the target cell genome with remarkable efficiency. Alternatively, delivery of genetic material may be accomplished using synthetic agents such as polyethylenimine (PEI)<sup>8</sup>, poly-L-lysine (PLL)<sup>9</sup>, polyamidoamine (PAMAM)<sup>10</sup>, chitosan<sup>11</sup> and various lipids such as 1,2-dioleoyl-3-trimethylammonium-propane (DOTAP)<sup>12</sup>, which electrostatically bind DNA or RNA and condense the nucleic acids to form nanoparticles<sup>7,13</sup>. These non-viral vectors typically offer improved safety, ease of targeting specific cells and facile manufacturing along with robust storage capabilities but are comparatively inefficient and typically provide short duration of gene expression<sup>14</sup>. Thus, both viral and non-viral vectors have significant advantages as well as limitations for application in human gene therapy. The design of hybrid viral/synthetic vectors provides a route to combine beneficial properties of conventional vectors, potentially leading to a superior vector with improved properties.

Retroviral-like particles (RVLP) lacking an envelope protein may be internalized via endocytosis but are incapable of transduction. We and others have demonstrated that the envelope protein which is responsible for initiating infection is also a prime reason for their disadvantages such as freeze-thaw instability, short half-life of infectivity (5-7 h at 37 °C) and difficult retargeting for receptor-specific gene therapy<sup>15-17</sup>. Replacing the envelope protein with a synthetic material has the potential to alleviate these limitations. For example, retroviruses have been associated with DOTAP and PEI in order to improve their transduction efficiency<sup>18,19</sup>. There have also been recent reports on non-covalently attaching GPI-anchored proteins and lipids to the retroviral lipid bilayer through novel post-insertion protocols<sup>20-22</sup>. These studies, however, required the presence of a functional envelope protein.

Our lab has previously reported the formation of hybrid vectors through non-covalent association of PEI or PLL with Moloney murine leukemia virus-like particles (M-VLP)<sup>15,23</sup>. In this article, we demonstrate the design of hybrid vectors through association of liposomes comprising DOTAP, DOPE (1,2-dioleoyl-*sn*-glycero-3-phosphoethanolamine) and cholesterol (hereafter referenced as  $\phi$ /M-VLP or  $\phi_{xyz}$ /M-VLP with composition DOTAP:DOPE:cholesterol = x:y:z on a weight basis). M-VLP on their own without envelope proteins or synthetic agents are incapable of achieving transduction in human cells.

DOTAP, a cationic lipid, has been used as a gene delivery vector for non-viral gene therapy<sup>24</sup> and viral gene therapy<sup>18,25</sup> since its first formulation in 1988<sup>12</sup>. Neutral “helper” lipids such as DOPE or cholesterol are commonly used with DOTAP in gene therapy applications to reduce the high cationic charge density and provide membrane fluidity for optimal performance<sup>26,27</sup>. DOPE is also believed to promote liposome fusion with the endosomal membrane through adoption of a hexagonal inverted phase (H<sub>II</sub>) structure thereby allowing efficient escape of the cargo into the cytosol<sup>26,28,29</sup>. Cholesterol has also been used as a significant component of lipid-based gene delivery vectors as a neutral, helper lipid<sup>27</sup> and in modified forms such as DC-Chol<sup>30</sup>. Here, we report highly efficient  $\phi$ /M-VLP-mediated transfection of mammalian cells with minimal toxicity along with stable long-term expression and vector stability.

## EXPERIMENTAL SECTION

### Cell Lines and Assays

Human embryonic kidney cells, HEK293, and human oral carcinoma cells, KB, were purchased from the American Type Culture Collection (Manassas, VA). The MLV producer

cell line, GP293Luc, containing the MLV viral *gag-pro-pol* genes and a construct comprising the MLV long-terminal repeats flanking a packaging sequence ( $\psi$ ) and neomycin resistance and luciferase reporter genes was purchased from Clontech (Mountain View, CA). All cell lines were grown in DMEM supplemented with 10% FBS and cultured at 37 °C in 5% CO<sub>2</sub>. Dulbecco's Modified Eagle's Medium (DMEM) and Phosphate-buffered saline (PBS) was produced in-house at the Cell Culture Media Facility, School of Chemical Sciences, University of Illinois. Fetal Bovine Serum (FBS) was bought from Gemini Bio-Products and used as purchased. Luciferase assay and Cell-Titer Blue™ assay kits were bought from Promega and used as per the manufacturer's instructions. BCA assay was bought from Thermo Scientific and used as per the manufacturer's instructions.

### M-VLP Production and Quantification

M-VLP were produced in GP293Luc cells ( $2 \times 10^6$ ) seeded in a 10 cm dish. The cells were cultured for four days before the M-VLP containing supernatant was collected and filtered through a 0.45  $\mu$ m surfactant-free cellulose acetate syringe filter. The concentration of M-VLP in the supernatant was measured using a q-RT-PCR protocol<sup>23</sup>. RNA Standards were obtained from the Clontech qPCR Retroviral Quantification Kit and stored at -80 °C before further use. Viral RNA was extracted using the QIAGEN Viral RNA Extraction kit and stored in a 60  $\mu$ l eluate at -80 °C before further use. Standards and viral RNA samples were prepared for reverse transcription using Taqman reverse transcription reagents (Applied Biosystems, Carlsbad, CA). Twenty  $\mu$ l samples were mixed in 200  $\mu$ l PCR tubes using the reagent concentrations suggested by the kit plus 250 nM sequence-specific primers. Thermal cycling was carried out on a Peltier Thermocycler (PTC)-100 (MJ Research). Real-time PCR of the cDNA standards and samples was carried out in triplicate in 10  $\mu$ l/well samples on a 384-well plate in a Taqman 7900 Real-Time PCR Machine (Applied Biosystems) and analyzed using SDS software (Applied Biosystems). The final reaction mixture ratio of the components was 5:1:1:3 (2X SYBRGreen real-time PCR reagent:forward primer:reverse primer:cDNA volume). The final concentration of the sample RNA was calculated using the calibration curve obtained via the cDNA standards. Each viral particle has 2 RNA copies which enabled us to calculate the total number of M-VLP in a given volume of supernatant. Two RNA extracts were collected for each M-VLP sample and quantified using 3 dilutions of each cDNA sample. M-VLP supernatant was either used immediately or stored at 4 °C for short term storage (< 4 weeks) or stored at -80 °C for long term storage.

### MLV-A Production

GP293Luc cells, seeded ( $2 \times 10^6$ ) in a 10 cm dish, were grown for 48 h prior to transfection with the envelope plasmid pMDM.4070A. Complete media was replaced with serum-free media just before transfections. The plasmid was conjugated with Lipofectamine2000 (LF2000) (Invitrogen, Carlsbad, CA) in a stoichiometric ratio of 1:5 (w:w) and incubated at room temperature for 10 min prior to drop-wise addition to GP293Luc cells. The media was replaced again with complete media 6 h post-transfection. The cells were cultured for a further 48 h before the MLV-A containing supernatant was collected and filtered through a 0.45  $\mu$ m surfactant-free cellulose acetate syringe filter.

### Synthesis of $\phi$ /M-VLP

Different strategies were tested for this study to optimize the formation of hybrid vectors in terms of their size and transfection efficiency.

### Protocol 1 (Dry Film Method)

The three lipids dissolved in chloroform were mixed in the desired composition in a test-tube and dried under vacuum overnight to form a thin film. The lipid film was rehydrated

using a 5% glucose solution and sonicated briefly to allow the lipids to dissolve completely. The rehydrated solution was vortexed every 30 minutes for 30 s for a total duration of 3 h. If not used immediately, the lipid solution was stored at 4 °C (< 1 month). The lipid samples were diluted in 5% glucose solution as per the required  $\phi$ /M-VLP stoichiometry followed by the addition of required volume of M-VLP supernatant and incubated for 2 h at 4 °C prior to further analysis or transfection.

### Protocol 2 (Multiple-Pass Extrusion without M-VLP)

The three lipids dissolved in chloroform were mixed in the desired composition in a test-tube and dried under vacuum overnight to form a thin film. The lipid film was rehydrated using a 5% glucose solution and sonicated briefly to allow the lipids to dissolve completely. The rehydrated solution was vortexed every 30 minutes for 30 seconds for a total duration of 3 h. If not used immediately, the lipid solution was stored at 4 °C (< 1 month). The lipid solution was extruded through an Avanti® Mini-Extruder for 11 passes through a 100 nm PC membrane. The lipid samples were diluted in 5% glucose solution as per the required  $\phi$ /M-VLP stoichiometry followed by the addition of required volume of M-VLP supernatant and incubated for 2 h at 4 °C prior to further analysis or transfection.

### Protocol 3 (Alcohol Injection)

The three lipids dissolved in chloroform were mixed in the desired composition in a test-tube and dried under vacuum overnight to form a thin film. The lipid film was resuspended in diethyl alcohol (with sonication if required). The alcohol solution was injected rapidly to the required volume of M-VLP supernatant and the alcohol was evaporated by establishing a vacuum line for solution for 4 h. The samples were stored at 4 °C prior to further analysis or transfections.

### Transfection by $\phi$ /M-VLP

$\phi$ /M-VLP were prepared as per the different protocols testing as part of this study. HEK293 and KB cells were seeded 18-24 h prior to transfection at  $4 \times 10^5$  cells/well in 12 well plates. Growth media containing serum was replaced with serum-free DMEM prior to drop-wise addition of vectors. DMEM was replaced with normal growth media 4 h post-transfection.

### Transduction by MLV-A

HEK293 cells were seeded 18-24 h prior to transduction at  $8 \times 10^4$  cells/well in 6-well plates. MLV-A containing supernatant was diluted in complete media (1:3, v:v) along with addition of 1  $\mu$ l Sequabrene for every 1 ml of the diluted mixture to produce viral media. HEK293 cells were transduced with 1 ml/well viral media.

### Luciferase expression assay

Luciferase expression was quantified 24-48 h post-transfection using the Promega luciferase assay system following the manufacturer's protocol. Luciferase activity was measured in relative light units (RLU) using a Lumat LB 9507 luminometer (Berthold, GmbH, Germany). Lysate protein concentration was then determined by BCA assay to standardize expression values.

### Cellular Uptake

20 ml of M-VLP supernatant was centrifuged at 60,000g for 2 h at 4 °C and the pellet was resuspended in 50 mM HEPES with 145 mM NaCl. 1,1'-dioctadecyl-3,3,3',3'-tetramethylindodicarbocyan-ine, 4-chlorobenzenesulfonate salt (DiD) (Invitrogen, 1 mM in DMSO, Ex = 644 nm, Em = 665 nm) was added to the resuspended M-VLP to give a final

concentration of 2  $\mu\text{M}$  DiD. The mixture was incubated for 1 h at room temperature. Labeled M-VLP were separated from the free dye through a PD-10 gel filtration desalting column (GE Healthcare). HEK293 cells were seeded in 12-well plates at  $4 \times 10^5$  cells per well 18-24 h prior to transfection. Hybrid vectors composed of liposomes and DiD-labeled M-VLP were synthesized as described above and transfected onto HEK293 cells. The target cells were washed with PBS containing 0.001% SDS 2 h post transfection to remove surface-bound, uninternalized vectors followed by a regular PBS wash. Cells were then trypsinized followed by neutralization with 50  $\mu\text{l}$  of FBS, collected, and analyzed by flow cytometry using a Becton Dickinson (Franklin Lakes, NJ) LSR II Flow Cytometer with a 633 nm laser.

### Negative Stain Transmission Electron Microscopy (TEM)

M-VLP and  $\phi$ /M-VLP were fixed by adding 1 ml of Karnovsky's fixative to 3 ml of sample. The sample was then centrifuged at 60,000g for 2 h at 4  $^{\circ}\text{C}$ . The pellet was resuspended in a small volume of 5% glucose and diluted with the fixative. A 40  $\mu\text{l}$  drop of the sample was placed on a parafilm sheet with a copper grid placed face down on the sample drop and incubated for 30 minutes. Excess sample was wicked off the grid using filter paper. The grid was then placed grid-face down on a drop of 7% uranyl acetate stain for 1 min. Excess stain was again wicked off using filter paper and the grid was dried for 15 min before viewing in a Hitachi H600 Transmission Electron Microscope.

### Size Measurements

$\phi$ /M-VLP were prepared as described above and diluted 10-fold in 5% glucose. The sizes of the resulting complexes and the constituents were measured using dynamic light scattering with a Brookhaven 90Plus Particle Size Analyzer (Brookhaven Instruments). Light scattering was measured 10 times at 10-second intervals for each sample.

### Surface Charge Measurements

M-VLP supernatant was centrifuged at 60,000g for 2 h at 4  $^{\circ}\text{C}$  and the pellet was resuspended in the same volume of 5% glucose.  $\phi$ /M-VLP were prepared as described above and diluted 5-fold in 5% glucose. The electrophoretic mobility of the resulting complexes and the constituents was measured using the ZetaPALS module attached to the Brookhaven 90Plus Particle Size Analyzer (Brookhaven Instruments) over 10 runs with 30 measurements per run. Zeta Potential was estimated using the Smoluchowski Equation.

### Cytotoxicity studies

The toxicity of liposomes was determined using the Cell Titer-Blue™ Cell Viability Assay. HEK293 cells were seeded in a 96-well plate at  $5 \times 10^4$  cells/well 18-24 h prior to addition of lipids. Liposomes formed in 5% glucose solutions via Protocol 1 were added to the cells in concentrations ranging from 0 (control) - 200 (maximum)  $\mu\text{g}/\text{ml}$  in serum-free medium and left for 4 h before the medium was replaced. Fifteen  $\mu\text{l}$  of CellTiter-Blue™ reagent was added to each well 24 h after the addition of polymers. The cells were incubated for further 4 h at 37  $^{\circ}\text{C}$  before adding 100  $\mu\text{l}$  per well of stop reagent following which fluorescence ( $\lambda = 570 \text{ nm}, 650 \text{ nm}$ ) was measured in a SpectraMax 340PC 96-well plate reader.  $\text{IC}_{50}$  = concentration at which cell viability is 50% of untreated cells.

### Stable Transgene Expression Assay

Hybrid vectors were formed as described above. HEK293 cells were seeded 18-24 h prior to transfection at  $8 \times 10^5$  cells/well in 6-well plates. Growth media containing serum was replaced with serum-free DMEM prior to drop-wise addition of vectors and replaced again with normal growth media 4 h post-transfection. After 48 h, the cells in three wells were

lysed and quantified for luciferase expression as mentioned above. The cells in the other three wells were split into another 6-well plate at a 1:8 split ratio. This process was repeated every 3-4 days depending on the confluency of the cells for up to at least three weeks.

### Statistical Analysis

All statistical analyses mentioned in this study was done using the Student's t-test.

## RESULTS

### Optimization of Lipid Composition for Efficient Transfection

For initial hybrid vector construction, multi-lamellar liposomes were produced by the dry-film method (Protocol 1)<sup>31</sup>. The liposomes were combined with M-VLP through simple mixing, which led to electrostatic interactions between the negatively-charged viral lipid bilayer and the positively-charged DOTAP head-group. HEK293 cells were transfected with  $\phi$ /M-VLP carrying the luciferase reporter gene at four lipid/M-VLP ratios of 4, 8, 12 and 16  $\mu\text{g}$  lipid/ $10^9$  M-VLP (Fig. 1). No measurable transgene expression was observed upon transfection with M-VLP in the absence of liposomes (not shown).

DOTAP-rich compositions performed poorly at all lipid/M-VLP ratios (lower right corner of triangle diagram). DOPE-heavy formulations also exhibited poor transfection efficiency (TE) overall (upper region of triangle). The best lipid compositions were those that contained 50% DOTAP and cholesterol-rich formulations with 10-40% DOPE content.  $\phi_{587}$ /M-VLP and  $\phi_{325}$ /M-VLP provided the greatest transfection efficiency amongst all the tested lipid compositions ( $\approx 1000$ -fold higher than the control, LF2000/M-VLP). For further characterization, control compositions –  $\phi_{505}$ /M-VLP and  $\phi_{550}$ /M-VLP – were also used along with  $\phi_{587}$ /M-VLP to compare the effects of the presence of either neutral helper lipid alone.

Transfection of KB cells was performed using the optimized lipid composition of  $\phi_{587}$ /M-VLP along with the controls,  $\phi_{505}$ /M-VLP and  $\phi_{550}$ /M-VLP (Fig. S1). Overall, the transfection efficiency was reduced in comparison to HEK293 cells by about 10-fold despite doubling of the viral particle load. The optimized composition of  $\phi_{587}$ /M-VLP exhibited higher transfection levels in comparison to the controls at high lipid:M-VLP ratios.

The transfection efficiency of  $\phi$ /M-VLP was also compared to transduction by MLV-A and PEI/M-VLP (Fig. S2). PEI/M-VLP were formed as reported previously<sup>32</sup>.  $\phi$ /M-VLP provided a higher transfection ability as compared to PEI/M-VLP (> ten-fold improvement) while its performance was comparable to transfection by MLV-A. The efficiency could also be further improved by modulating the lipid weight used for complexing M-VLPs.

### Cellular Uptake of $\phi$ /M-VLP in HEK293 cells

It is also informative to investigate the effects of the different lipid compositions on the cellular uptake of the vectors (Fig. 2). While the presence of DOTAP was expected to be necessary to mediate cellular uptake via electrostatic interactions with the cell surface, it was important to understand the impact of the presence of DOPE and cholesterol on cellular uptake. M-VLP tagged with the lipophilic fluorescent dye DiD were complexed with the liposomes of desired composition at 5, 10 and 20  $\mu\text{g}$ / $10^9$  M-VLP. In order to compare the effect of all three lipids, we used the following lipid compositions:  $\phi_{100}$ /M-VLP,  $\phi_{550}$ /M-VLP and  $\phi_{587}$ /M-VLP, which represented DOTAP in decreasing proportion.  $\phi_{100}$ /M-VLP exhibited the highest mean cellular fluorescence at all lipid/M-VLP ratios followed by  $\phi_{550}$ /M-VLP and  $\phi_{587}$ /M-VLP. This was significant considering that cationic DOTAP-rich lipids were amongst the least efficient in transfections (Fig. 1). In fact, the transfection efficiency

mediated by  $\phi_{100}$ /M-VLP,  $\phi_{550}$ /M-VLP and  $\phi_{587}$ /M-VLP was inversely correlated to the uptake. Therefore, it appears that cellular uptake represents a minor barrier in the transfection mechanism of  $\phi$ /M-VLP. Additionally, even though M-VLP are incapable of transduction, minor fluorescence shift measured with samples transfected with M-VLP alone indicates that they may be internalized and trapped within endocytic vesicles.

### Toxicity of DOTAP, DOPE and cholesterol liposomes on HEK293 cells

The toxicity of DOTAP/DOPE/cholesterol liposomes on HEK293 cells was measured to determine if it affected the transfection efficiency, especially at higher lipid/M-VLP ratios (Fig. 3). Both  $\phi_{550}$  and  $\phi_{587}$  exhibited almost no toxic effect up to concentrations of 150  $\mu\text{g/ml}$  whereas the cell viability was reduced to <80% for  $\phi_{505}$  at concentrations >25  $\mu\text{g/ml}$  with an  $\text{IC}_{50}$  >100  $\mu\text{g/ml}$ . Considering that  $\phi_{505}$  exhibited mild toxicity, it was surprising that  $\phi_{587}$  showed no deleterious effects on the cells despite the presence of cholesterol. This observation may be explained by the presence of DOPE in  $\phi_{587}$  that may have led to an efficient trafficking mechanism and/or exocytosis of the lipids leading to lower toxicity. The maximum concentration of liposomes used in the transfection and uptake studies was <25  $\mu\text{g/ml}$ . Hence, it is clear that the toxicity of these lipids had negligible influence on the overall transfection efficiency, trafficking and uptake of the vectors in HEK293 cells.

### Alternate Approaches for $\phi$ /M-VLP Formation

The dry-film method for preparation of liposomes (Protocol 1) allowed for the rapid, simultaneous testing of different liposome compositions for optimal transfection efficiency. The sizes of the hybrid vectors as measured via dynamic light scattering (DLS), however, varied from 300 nm to >1  $\mu\text{m}$  and were much larger than the M-VLP ( $93 \pm 4$  nm) (Table 1 and Fig. 4a), especially at higher lipid/M-VLP ratios ( $10 \mu\text{g}/10^9$  M-VLP), suggesting aggregation of multiple M-VLP in individual complexes. Such aggregation of these hybrid vectors was visualized via transmission electron microscopy (TEM) (Fig. 4c), which correlated well with the sizes measured via DLS. The large size suggested that an alternative method of constructing the hybrid vectors would be desirable. Hence, we tested various methods that have been used in liposomal gene and drug delivery protocols to reduce vector sizes, of which two that provided the best results are reported here.

In Protocol 2, we used extrusion to produce significantly smaller liposomes of 130-180 nm (Fig. 4b and Table 1)<sup>33</sup>. The sizes of the hybrid vectors containing extruded liposomes were much smaller (200-400 nm) as compared to the  $\approx 1000$  nm sizes of  $\phi$ /M-VLP formed with liposomes prepared via Protocol 1. Visualization via TEM (Fig. 4d) further revealed  $\phi$ /M-VLP containing liposomes formed via Protocol 2 wherein the lipid bilayer (solid white arrows) appeared to surround the M-VLP (solid black arrows).

The alcohol injection method, Protocol 3, has been used to prepare large liposomes for encapsulating proteins, mRNA, siRNA and DNA<sup>34-37</sup>. Lipids dissolved in ethanol were injected rapidly into an aqueous solution containing M-VLP and upon evaporation of alcohol under vacuum led to a slow transfer of lipids into the aqueous phase forming hybrid vectors. This protocol suffered from precipitation of the lipids upon evaporation of alcohol except when preparing  $\phi_{550}$ /M-VLP. However, the sizes of the hybrid vectors were smaller than those formed via Protocol 2 at 10 and 20  $\mu\text{g}/10^9$  M-VLP (Table 1). TEM showed the lipid (white arrow) enveloping the M-VLP (black arrow), suggesting that the smaller sizes of these vectors are due to not just the presence of smaller liposomal structures formed during the transfer of the lipid from the lipid/alcohol to the aqueous phase, but also the association of the lipid with M-VLP (Fig. 4e).

The transfection efficiency of  $\phi$ /M-VLP formed via Protocols 2 and 3 compared to Protocol 1 was also investigated (Fig. 5). TE decreased by 33% for  $\phi_{587}$ /M-VLP prepared via Protocol 2 (Fig. 5a) at the optimal lipid stoichiometry. TE also decreased by 33% for  $\phi_{550}$ /M-VLP (Fig. S3) and increased by 33% for  $\phi_{505}$ /M-VLP (Fig. S4) prepared via Protocol 2. Transfection with  $\phi_{550}$ /M-VLP prepared via Protocol 3, in contrast, was poor as compared to those formed using Protocol 1 (Fig. 5b, 20-fold lower,  $p < 0.005$ ). While transfection of these hybrid vectors improved as the percentage of ethanol in the M-VLP solution decreased, any further reduction in alcohol content below 8% led to no more improvements in transfections. Previous studies have suggested that DOPE-rich cationic liposomes prepared by this method are optimal non-viral gene delivery vectors (with plasmid DNA) with better transfection efficiency and size stability as compared to the dry-film method used in Protocol 1<sup>37</sup>. However, liposomes were formed by this method prior to conjugation with DNA via simple mixing whereas in our study the hybrid vectors were formed with this method rather than just the liposomes. It is evident that this protocol led to minimal aggregation thereby forming smaller vectors, but ethanol may have deactivated the virus, for example by fixing.

The sizes of  $\phi$ /M-VLP formed via Protocol 1 can be reduced further via decrease in the stock concentration of the lipid used to form the hybrid vectors (Table S1). However, the transfection efficiency decreased with decreasing lipid concentration (Fig. S5). Additionally, the optimal lipid/M-VLP ratio required for efficient transfection changed with the lipid concentration from  $10 \mu\text{g}/10^9$  M-VLP at 1 mg/ml to  $17.5 \mu\text{g}/10^9$  M-VLP at 0.5 mg/ml and  $12.5\text{-}20 \mu\text{g}/10^9$  M-VLP at 0.25 mg/ml. The significant difference in the transfection efficiency at 5 and  $10 \mu\text{g}/10^9$  M-VLP at the three different lipid concentrations was surprising. One possible reason could be the time required for complexation of M-VLP and lipids. Low lipid concentrations may require more time for forming effective hybrid structures than the high concentration solutions. This might also lead to a greater presence of free lipid in solution that remained unassociated with the M-VLP leading to sub-optimal hybrid vector formation.

### Effect of Long-Term Storage on Vector Size and Transfection Efficiency

The  $t_{1/2}$  of infectivity for MLV-A (amphotropic murine leukemia virus) is 5-7 h at  $37^\circ\text{C}$ <sup>16</sup>. MLVs are known to be unstable upon storage for  $>4$  days even at low temperatures ( $4^\circ\text{C}$ )<sup>16,23,32</sup>. Previous studies have shown that the envelope protein is one of the reasons for poor MLV stability<sup>17,38,39</sup>. In fact, the stability of these viruses can be strongly modulated through the pseudotyping of different envelope proteins. For example, the retroviruses with the VSV-G envelope protein can be stored at  $4^\circ\text{C}$  for several weeks. In contrast, M-VLP alone exhibit good long-term storage stability<sup>23</sup>. M-VLP stored at  $4^\circ\text{C}$  (14 days) used to produce hybrid vectors maintained their transfection efficiency whereas storage of MLV-A ( $>4$  days at  $4^\circ\text{C}$ ) led to poor transduction ( $<1\%$ ). In this study, we extended the storage studies to preformed  $\phi$ /M-VLP stored at  $4^\circ\text{C}$  for 12 days (Fig. 6). Both TE as well as the size of the hybrid vectors was measured over the testing period. TE of MLV-A underwent drastic reduction by over 99% over the 12 days while the size of MLV-A did not change.

The size of  $\phi_{505}$ /M-VLP remained fairly stable except for a minor decrease at  $10 \mu\text{g}/10^9$  M-VLP. After 12 days, the TE of  $\phi_{505}$ /M-VLP at  $5 \mu\text{g}/10^9$  M-VLP increased three-fold, but at  $10 \mu\text{g}/10^9$  M-VLP decreased three-fold. The reduction in TE at the higher stoichiometry could be attributed to the observed size decrease via possible dissociation of the liposomes from the M-VLP. The size of  $\phi_{550}$ /M-VLP varied significantly over the 12-day period. However, the TE decreased to  $<20\%$  after 12 days. The size of  $\phi_{587}$ /M-VLP remained fairly stable over the 12-day period but TE decreased to  $<30\%$  of TE on day 0. Despite fairly robust stability in size of  $\phi_{587}$ /M-VLP and  $\phi_{550}$ /M-VLP, TE decreased uniformly over the same period.



## Long Term Stable Transfections

MLV is capable of stable transduction due to integration of the transgene into the target cell genome. It is expected that once the core viral particle enters a cell as an intact virion or a hybrid vector, genome integration and stable transgene expression should be achieved. Past studies have shown that hybrid vectors comprising polymers were indeed capable of stable transfections<sup>32</sup>. Thus, we explored the stability of transgene expression upon transfection with  $\phi$ /M-VLP hybrid vectors (Fig. 7).  $\phi$ /M-VLP were able to successfully provide stable expression over at least three weeks. From Fig. 3, we know that  $\phi_{505}$ /M-VLP can be toxic at very high concentrations. However, since in the transfections reported here cells were exposed to negligibly toxic lipid concentrations  $<10 \mu\text{g/ml}$ , transfections were efficient and stable.

## DISCUSSION

Rescue of M-VLP infectivity using lipids has been reported previously. One of the first studies used proprietary lipid formulations such as Lipofectin, Cellfectin, Lipofectamine and Transfectamine<sup>40</sup>. M-VLP were either incubated with these reagents prior to transfection or were added to target cells that were pre-incubated with the transfection reagents. Other similar work employed DOTAP and DC-Chol:DOPE (3:2) liposomes<sup>18,41</sup>. In the present study, we expanded upon these previous attempts in two ways. We optimized the lipid composition for the synthetic envelope using a ternary mixture of DOTAP, DOPE and cholesterol. Secondly, we further optimized the vector morphology by controlling the liposome sizes to obtain individual hybrid vectors rather than aggregates – an issue that hampered both the studies mentioned above as well as our polymer-based hybrid vectors, thereby allowing the possibility of systemic *in vivo* gene delivery<sup>32</sup>. We also demonstrated that the same optimized lipid composition shows high transfection capabilities in other cell lines such as KB cancer cells. The hybrid vectors also exhibited performance comparable to MLV-A, which is known to have high transduction efficiency in HEK293 cells owing to its amphotropic envelope protein, suggesting the potential of these vectors for *in vivo* testing.

DOTAP, the cationic lipid, was required as part of the lipid composition (DOPE:cholesterol  $\phi$ /M-VLP with no DOTAP were unable to transfect HEK293 cells; data not shown). The three lipids also differed in their packing in self-assembled structures. DOTAP prefers the  $L_{\alpha}$  phase whereas DOPE and cholesterol prefer the  $H_{II}$  inverted phase since  $P$  (critical lipid packing parameter)  $<1$  for DOTAP and  $>1$  for DOPE and cholesterol at the temperatures of interest to this study (0-40 °C)<sup>42,43</sup>. Phase changes can also take place due to changes in lipid compositions or external factors such as salt composition and pH<sup>44,45</sup>.

The lipid composition affected the size and charge of  $\phi$ /M-VLP. The presence of DOPE in  $\phi_{550}$ /M-VLP and  $\phi_{587}$ /M-VLP led to larger vector sizes especially at higher lipid/M-VLP ratios. During the formation of these lipid vectors, it is likely that the presence of DOPE led to the formation of the  $H_{II}$  phase much more effectively than cholesterol. This would explain the fact that  $\phi_{550}$ /M-VLP were larger in size at very high lipid ratios due to a higher degree of inverted phase structures. It may also explain why  $\phi_{550}$ /M-VLP had a lower zeta potential at  $20 \mu\text{g}/10^9$  M-VLP compared to  $10 \mu\text{g}/10^9$  M-VLP (Table S1). The change in zeta potential with respect to lipid/M-VLP ratios was steeper in  $\phi_{587}$ /M-VLP than in  $\phi_{505}$ /M-VLP, suggesting that the outer surface was cholesterol-rich in lipid formulations containing only cholesterol (Table S1). This is also supported by other studies that demonstrate the presence of cholesterol nano-domains in cholesterol-rich lipid-based formulations<sup>46</sup>.

The potential for formation of the inverted  $H_{II}$  phase is known to be an important parameter for optimal transfection efficiency of lipid-based gene delivery vectors<sup>47,48</sup>. The very low transfection efficiency of  $\phi_{100}$ /M-VLP could be explained by the expectation that almost the

entire hybrid vector was in  $L_{\alpha}$  phase with very minimal potential for enabling the  $H_{II}$  phase during transfections. Additional transition from  $L_{\alpha}$  to  $H_{II}$  would be expected to occur only within the cellular microenvironment in acidified vesicles. It is known that both cholesterol<sup>42,43,47</sup> and DOPE<sup>42,44,47</sup> enable the transition from lamellar to inverted phase within endosomes. As seen in Figs. 5, S3 and S4, the optimal lipid stoichiometry for efficient transfection decreased with increased DOPE content in the lipid formulation. It is possible that DOPE favored the inverted phase structure to a greater degree and at lower lipid/M-VLP ratios compared to cholesterol thereby enabling quicker release of M-VLP into the cytosol. It is also likely that the DOPE-based vectors were already oriented to a certain degree in  $H_{II}$  phase, which can be inferred from the larger vector sizes in DOPE-containing vectors at high lipid/M-VLP ratios as well as the zeta potential of the lipids alone (Table S1, 5:0:5 exhibited higher zeta potential than 5:5:0 despite the presence of the same amount of DOTAP). Hence, any higher lipid/M-VLP ratios in DOPE-based vectors led to loosely-condensed M-VLP that did not perform as efficiently as compared to lower lipid/M-VLP ratios due to poor vector morphology (Fig. S3). At the same time, a greater amount of cholesterol was required to achieve the desired inverted phase structure for optimal vector morphology as well as optimal release of the M-VLP within the cytosol, which explains the larger lipid/M-VLP ratios required for efficient transfections (Fig. S4). For  $\phi_{587}$ /M-VLP the optimal transfection efficiency was between that of  $\phi_{550}$ /M-VLP and  $\phi_{505}$ /M-VLP which was surprising given that the presence of both the neutral helper lipids promoting the inverted phase structure would enable efficient transfections at lower lipid/M-VLP ratios (Fig. 5).

It is probable that the mechanism of phase inversion differs for the two neutral species, however. The likely neutral helper lipid to initiate this transition would be DOPE, but due to its lower proportion as compared to  $\phi_{550}$ /M-VLP the optimal transfection efficiency was achieved at higher lipid/M-VLP ratios. Additionally, the transition temperature for DOPE from  $L_{\alpha}$  to  $H_{II}$  is predicted to be between 9-18° C which is surpassed upon transfection at 37 °C<sup>49</sup>. Upon long-term storage at 4 °C, it is possible that the association between M-VLP and liposomes is weakened or the liposome/M-VLP complexes are disrupted due to the inherent leaky nature of the liposomes. This may explain why both  $\phi_{587}$ /M-VLP and  $\phi_{550}$ /M-VLP exhibited a significant decrease in transfection activity after the 12-day period at 4 °C (Fig. 6). In contrast, transfection with  $\phi_{505}$ /M-VLP was maintained or improved, most likely due to their increased stability. It is known that cholesterol improves the stability of liposomes both *in vivo* and *in vitro*<sup>50</sup>.

The development of viral/synthetic hybrid vectors represents a novel paradigm in the development of gene therapy vectors. However, we recognize limitations in our design which need to be resolved prior to further translational research. The use of retroviruses itself is a primary bottleneck since it limits the application to actively dividing cells. The use of lentiviral-like particles as shown earlier by our group along enabled the application of this novel design in non-dividing cells as well<sup>32</sup>. Secondly, both liposomes and M-VLPs are known to be unstable, and further work needs to be done to study these systems on varying conditions of storage and buffer compositions. The current design of these vectors relies on non-specific electrostatic attraction between the lipids, M-VLPs and cells for vector formation and cell uptake. While this is a disadvantage if systemic gene therapy is the ultimate application, incorporation of lipids containing targeting ligands such as folate, mannose or other ligands in the lipid mixture may achieve the desired cell or tissue specificity. Further, lipids containing polyethylene glycol or other hydrophilic polymers in the headgroup may provide longer retention times within circulation. Novel oncolytic vectors could be designed using this approach wherein folate-targeted lipids could be added to the lipid mixture and associated with retroviruses/lentiviruses reprogrammed with

oncolytic genes to specifically target cancer cells. Genetically or chemically modifying the envelope protein with folate molecules resulted in inefficient vectors<sup>51</sup>.

Overall,  $\phi$ /M-VLP formed via Protocol 2 exhibited the smallest sizes and the highest transfection efficiencies. Conversely, larger vectors led to relatively poor transfections. Additionally, we conclude that lipids which promoted the formation of the H<sub>II</sub> phase at the appropriate lipid/M-VLP ratios as well as the right time during transfection provided the most optimal transfections. We suggest that the optimal liposome composition and lipid/M-VLP ratio were such that the hybrid vector structure was on the verge of arranging in the H<sub>II</sub> phase which then occurred during transfection in the appropriate vesicles within the cellular microenvironment and allowed the M-VLP to progress through the remainder of the infection process including provirus formation and genomic integration.

## Supplementary Material

Refer to Web version on PubMed Central for supplementary material.

## Acknowledgments

This work was partially supported by the National Science Foundation (BES 06-02636) and National Institutes of Health GM085222. In addition, we thank Sandra Mattick at the Cell Culture Media Facility for help with preparation of cell media. Flow cytometry was performed at the Roy J. Carver Biotechnology Center Flow Cytometry Facility. TEM was performed with the assistance of Lou Ann Miller at the Frederick Seitz Materials Research Laboratory, University of Illinois. q-RT-PCR was performed at the Institute of Genomic Biology Core Facilities, University of Illinois.

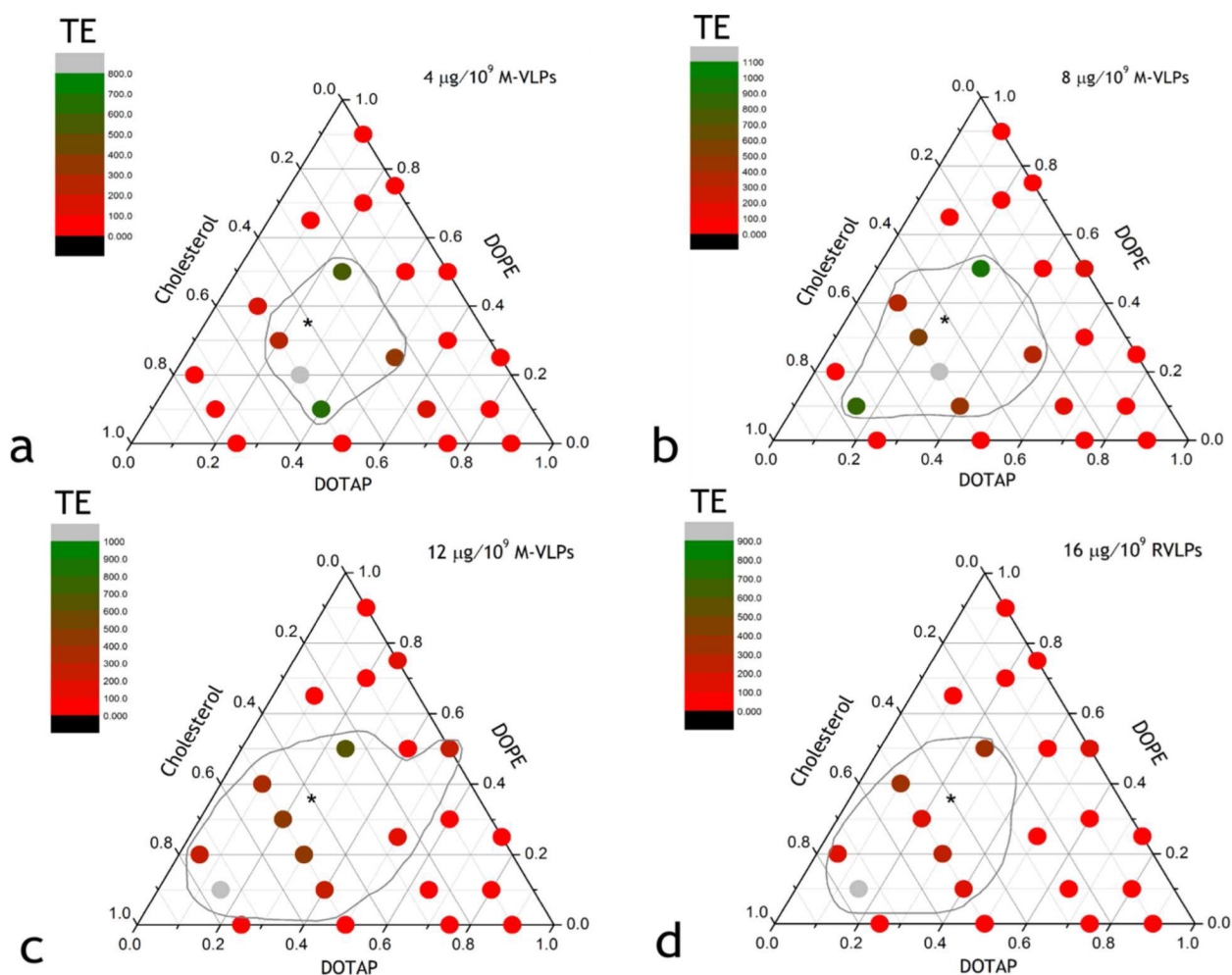
Additional data on size and zeta potential of  $\phi$ /M-VLP,  $\phi$ /M-VLP transfection of KB cells, comparison of  $\phi$ /M-VLP and PEI/M-VLP transfection, comparison of transfection with  $\phi$ /M-VLP formed via the dry film method versus extrusion, and the effect of liposome concentration of transfection with  $\phi$ /M-VLP. This information is available free of charge via the Internet at <http://pubs.acs.org/>.

## REFERENCES

1. Alton E, Ferrari S, Griesenbach U. Progress and Prospects: Gene Therapy Clinical Trials (Part 1). *Gene Ther.* 2007; 14:1439–47. [PubMed: 17909539]
2. Odom GL, Gregorevic P, Chamberlain JS. Viral-Mediated Gene Therapy for the Muscular Dystrophies: Successes, Limitations and Recent Advances. *Biochim. Biophys. Acta.* 2007; 1772:243–62. [PubMed: 17064882]
3. Galanis E, Russell S. Cancer Gene Therapy Clinical Trials: Lessons for the Future. *Br. J. Cancer.* 2001; 85:1432–6. [PubMed: 11720424]
4. Alton E, Ferrari S, Griesenbach U, Aiuti A, Bachoud-Lévi AC, Blesch A, Brenner MK, Cattaneo F, Chioccia E. a, Gao G, High K. a, Leen a M, Lemoine NR, McNeish I. a, Meneguzzi G, Peschanski M, Roncarolo MG, Strayer DS, Tuszynski MH, Waxman DJ, Wilson JM. Progress and Prospects: Gene Therapy Clinical Trials (Part 2). *Gene Ther.* 2007; 14:1555–63. [PubMed: 17984995]
5. McCarthy M. Gene Therapy Applied to Treatment of HIV-1 Infection. *Lancet.* 1998; 351:1709. [PubMed: 9734898]
6. Verma IM, Somia N. Gene Therapy -- Promises, Problems and Prospects. *Nature.* 1997; 389:239–42. [PubMed: 9305836]
7. Pack DW, Hoffman AS, Pun S, Stayton PS. Design and Development of Polymers for Gene Delivery. *Nat. Re. Drug Discov.* 2005; 4:581–593.
8. Boussif O, Lezoualc'h F, Zanta MA, Mergny MD, Scherman D, Demeneix B, Behr JP, A, Behr A. A Versatile Vector for Gene and Oligonucleotide Transfer into Cells in Culture and In Vivo: Polyethylenimine. *Proc. Natl. Acad. Sci. U.S.A.* 1995; 92:7297–7301. [PubMed: 7638184]
9. Erbacher P, Bousser M-T, Raimond J, Monsigny M, Midoux P, Roche AC. Transfer by DNA/Glycosylated Polylysine Complexes into Human Blood Monocyte-Derived. *Hum. Gene Ther.* 1996; 7:721–729. [PubMed: 8919594]

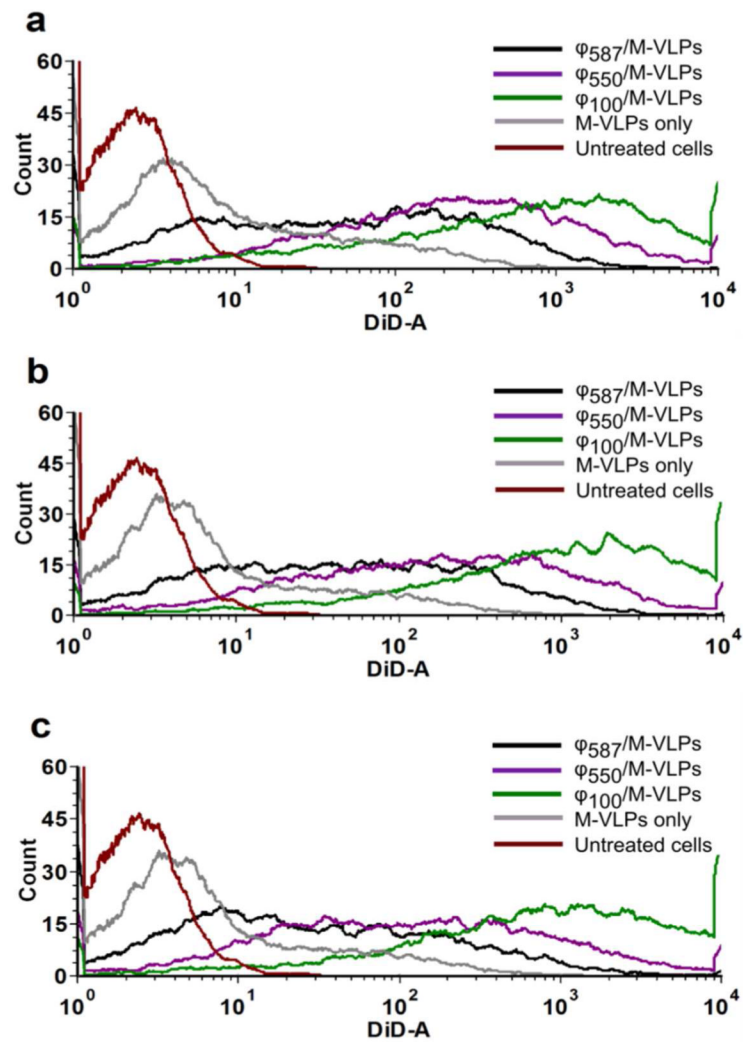
10. Haensler J, Szoka FC. Polyamidoamine Cascade Polymers Mediate Efficient Transfection of Cells in Culture. *Bioconjug. Chem.* 1993; 4:372–9. [PubMed: 8274523]
11. Jayakumar R, Chennazhi KP, Muzzarelli RAA, Tamura H, Nair SV, Selvamurugan N. Chitosan Conjugated DNA Nanoparticles in Gene Therapy. *Carbohydr. Polym.* 2010; 79:1–8.
12. Stamatatos L, Leventis R, Zuckermann MJ, Silvius JR. Interactions of Cationic Lipid Vesicles with Negatively Charged Phospholipid Vesicles and Biological Membranes. *Biochem.* 1988; 27:3917–25. [PubMed: 3415963]
13. Mairhofer J, Grabherr R. Rational Vector Design for Efficient Non-Viral Gene Delivery: Challenges Facing the Use of Plasmid DNA. *Mol. Biotechnol.* 2008; 39:97–104. [PubMed: 18327557]
14. Li S, Huang L. Nonviral Gene Therapy: Promises and Challenges. *Gene Ther.* 2000; 7:31–4. [PubMed: 10680013]
15. Ramsey JD, Vu HN, Pack DW. A Top-Down Approach for Construction of Hybrid Polymer-Virus Gene Delivery Vectors. *J. Controlled Release.* 2010; 144:39–45.
16. Vu HN, Ramsey JD, Pack DW. Engineering of a Stable Retroviral Gene Delivery Vector by Directed Evolution. *Mol. Ther.* 2008; 16:308–314. [PubMed: 17984974]
17. Lee GM, Choi JH, Jun SC, Palsson BO. Temperature Significantly Affects Retroviral Vector Production and Deactivation Rates, and Thereby Determines Retroviral Titers. *Bioprocess Eng.* 1998; 19:343–49.
18. Porter C, Lukacs KV, Box G, Takeuchi Y, Collins MKL. Cationic Liposomes Enhance the Rate of Transduction by a Recombinant Retroviral Vector In Vitro and In Vivo. *J. Virol.* 1998; 72:4832–4840. [PubMed: 9573249]
19. Themis M, Forbes SJ, Chan L, Cooper RG, Etheridge CJ, Miller AD, Hodgson HJ, Coutelle C. Enhanced In Vitro and In Vivo Gene Delivery Using Cationic Agent Complexed Retrovirus Vectors. *Gene Ther.* 1998; 5:1180–6. [PubMed: 9930318]
20. Mukherjee NG, Lyon LA, Le Doux JM. Rapid Modification of Retroviruses Using Lipid Conjugates. *Nanotechnology.* 2009; 20:065103. [PubMed: 19417371]
21. Metzner C, Mostegl MM, Günzburg WH, Salmons B, Dangerfield JA. Association of Glycosylphosphatidylinositol-Anchored Protein with Retroviral Particles. *FASEB J.* 2008; 22:2734–9. [PubMed: 18477763]
22. Metzner C, Salmons B, Günzburg WH, Dangerfield JA. Rafts, Anchors and Viruses--a Role for Glycosylphosphatidylinositol Anchored Proteins in the Modification of Enveloped Viruses and Viral Vectors. *Virol.* 2008; 382:125–31.
23. Drake DM, Keswani RK, Pack DW. Effect of Serum on Transfection by Polyethylenimine/Virus-Like Particle Hybrid Gene Delivery Vectors. *Pharm. Res.* 2010; 27:2457–2465. [PubMed: 20730559]
24. Hodgson CP, Solaiman F. Virosomes: Cationic Liposomes Enhance Retroviral Transduction. *Nat. Biotechnol.* 1996; 14:339–342. [PubMed: 9630897]
25. Singh R, Al-jamal KT, Lacerda L, Kostarelos K. Nanoengineering Artificial Lipid Envelopes Around Adenovirus by Self-Assembly. *ACS Nano.* 2008; 2:1040–1050. [PubMed: 19206502]
26. Balazs DA, Godbey WT. Liposomes for Use in Gene Delivery. *J. Drug Deliv.* 2011; 2011:326497. [PubMed: 21490748]
27. Crook K, Stevenson BJ, Dubouchet M, Porteous DJ. Inclusion of Cholesterol in DOTAP Transfection Complexes Increases the Delivery of DNA to Cells In Vitro in the Presence of Serum. *Gene Ther.* 1998; 5:137–43. [PubMed: 9536275]
28. Xu L, Anchordoquy T. Drug Delivery Trends in Clinical Trials and Translational Medicine: Challenges and Opportunities in the Delivery of Nucleic Acid-Based Therapeutics. *J. Pharm. Sci.* 2010; 100:38–52. [PubMed: 20575003]
29. Pichon C, Billiet L, Midoux P. Chemical Vectors for Gene Delivery: Uptake and Intracellular Trafficking. *Curr. Opin. Biotechnol.* 2010; 21:640–645. [PubMed: 20674331]
30. Gao X, Huang L. A Novel Cationic Liposome Reagent for Efficient Transfection of Mammalian Cells. *Biochem. Biophys. Res. Comm.* 1991; 179:280–285. [PubMed: 1883357]
31. Bangham AD, Standish MM, Watkins JC. Diffusion of Univalent Ions Across the Lamellae of Swollen Phospholipids. *J. Mol. Biol.* 1965; 13:238–52. [PubMed: 5859039]

32. Ramsey JD, Vu HN, Pack DW. A Top-Down Approach for Construction of Hybrid Polymer-Virus Gene Delivery Vectors. *J. Controlled Release*. 2010; 144:39–45.
33. MacDonald RC, MacDonald RI, Menco BP, Takeshita K, Subbarao NK, Hu LR. Small-Volume Extrusion Apparatus for Preparation of Large, Unilamellar Vesicles. *Biochim. Biophys. Acta*. 1991; 1061:297–303. [PubMed: 1998698]
34. Szoka F. Procedure for Preparation of Liposomes with Large Internal Aqueous Space and High Capture by Reverse-Phase Evaporation. *Proc. Natl. Acad. Sci. U.S.A.* 1978; 75:4194–4198. [PubMed: 279908]
35. Batzri S, Korn ED. Single Bilayer Liposomes Prepared without Sonication. *Biochim. Biophys. Acta*. 1973; 298:1015–1019. [PubMed: 4738145]
36. Zhou C, Mao Y, Sugimoto Y, Zhang Y, Kanthamneni N, Yu B, Brueggemeier RW, Lee LJ, Lee RJ. SPANosomes as Delivery Vehicles for Small Interfering RNA (siRNA). *Mol. Pharm.* 2012; 9:201–10. [PubMed: 22149175]
37. Maitani Y, Igarashi S, Sato M, Hattori Y. Cationic Liposome (DC-Chol/DOPE=1:2) and a Modified Ethanol Injection Method to Prepare Liposomes, Increased Gene Expression. *Int. J. Pharm.* 2007; 342:33–9. [PubMed: 17566677]
38. Andreadis ST, Roth CM, Doux L, J.m, Morgan JR, Yarmush ML, Le Doux JM. Large-Scale Processing of Recombinant Retroviruses for Gene Therapy. *Biotechnol. Prog.* 1999; 15:1–11. [PubMed: 9933508]
39. Richardson TB, Porter CD. Inactivation of Murine Leukaemia Virus by Exposure to Visible Light. *Virology*. 2005; 341:321–9.
40. Sharma S, Murai F, Miyanojara A, Friedmann T. Noninfectious Virus-Like Particles Produced by Moloney Murine Leukemia Virus-Based Retrovirus Packaging Cells Deficient in Viral Envelope Become Infectious in the Presence of Lipofection Reagents. *Proc. Natl. Acad. Sci. U.S.A.* 1997; 94:10803–8. [PubMed: 9380714]
41. Porter CD. Rescue of Retroviral Envelope Fusion Deficiencies by Cationic Liposomes. *J Gene Med.* 2002; 4:622–33. [PubMed: 12439854]
42. Simberg D, Danino D, Talmon Y, Minsky A, Ferrari ME, Wheeler CJ, Barenholz Y. Phase Behavior, DNA Ordering, and Size Instability of Cationic Lipoplexes. Relevance to Optimal Transfection Activity. *J. Biol. Chem.* 2001; 276:47453–9. [PubMed: 11564736]
43. Tilcock CP, Bally MB, Farren SB, Cullis PR. Influence of Cholesterol on the Structural Preferences of Dioleoylphosphatidylethanolamine-Dioleoylphosphatidylcholine Systems: a Phosphorus-31 and Deuterium Nuclear Magnetic Resonance Study. *Biochem.* 1982; 21:4596–601. [PubMed: 7138819]
44. Zuhorn IS, Engberts JBFN, Hoekstra D. Gene Delivery by Cationic Lipid Vectors: Overcoming Cellular Barriers. *Euro. Biophys. J.* 2007; 36:349–62.
45. Hsu W-L, Chen H-L, Liou W, Lin H-K, Liu W-L. Mesomorphic Complexes of DNA with the Mixtures of a Cationic Surfactant and a Neutral Lipid. *Langmuir*. 2005; 21:9426–31. [PubMed: 16207017]
46. Xu L, Anchordoquy TJ. Effect of Cholesterol Nanodomains on the Targeting of Lipid-Based Gene Delivery in Cultured Cells. *Mol. Pharm.* 2010; 7:1311–7. [PubMed: 20568694]
47. Hafez IM, Maurer N, Cullis PR. On the Mechanism Whereby Cationic Lipids Promote Intracellular Delivery of Polynucleic Acids. *Gene Ther.* 2001; 8:1188–96. [PubMed: 11509950]
48. Regelin AE, Fankhaenel S, Gurtesch L, Prinz C, Von Kiedrowski G, Massing U. Biophysical and Lipofection Studies of DOTAP Analogs. *Biochim. Biophys. Acta*. 2000; 1464:151–64. [PubMed: 10704929]
49. Shalaev EY, Steponkus PL. Phase Diagram of 1,2-Dioleoylphosphatidylethanolamine (DOPE):Water System at Subzero Temperatures and at Low Water Contents. *Biochim. Biophys. Acta*. 1999; 1419:229–47. [PubMed: 10407074]
50. Kirby C, Clarke J, Gregoriadis G. Effect of the Cholesterol Content of Small Unilamellar Liposomes on Their Stability In Vivo and In Vitro. *Biochem. J.* 1980; 186:591–8. [PubMed: 7378067]
51. Reddy, J. a; Clapp, DW.; Low, PS. Retargeting of Viral Vectors to the Folate Receptor Endocytic Pathway. *J. Controlled Release*. 2001; 74:77–82.

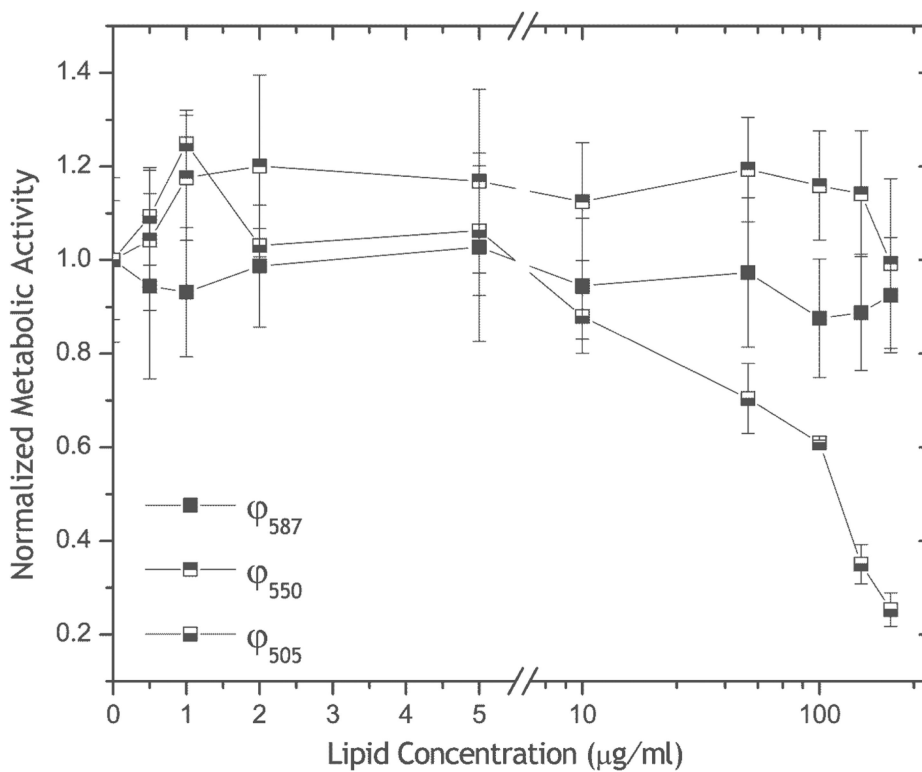


**Figure 1.**

Ternary plots of HEK293 cell transfection mediated by hybrid vectors comprising lipid formulations of DOTAP, DOPE and cholesterol. Each axis on the ternary plot represents one of the lipid components from 0% to 100% weight basis. The color of the dots represents the improvement of TE (from red to green). (a)  $4 \mu\text{g lipid}/10^9 \text{ M-VLP}$ , (b)  $8 \mu\text{g lipid}/10^9 \text{ M-VLP}$ , (c)  $12 \mu\text{g lipid}/10^9 \text{ M-VLP}$  and (d)  $16 \mu\text{g lipid}/10^9 \text{ M-VLP}$ . TE = transfection of  $\phi/\text{M-VLP}$  normalized to LF2000/M-VLP at  $5 \mu\text{g lipid}/10^9 \text{ M-VLP}$ . The grey contour line in each plot indicates lipid compositions that exhibited TE > 100. Transfection data were obtained with delivery of  $1 \times 10^9 \text{ M-VLP/well}$  of a 12-well tissue culture plate with vector formation using M-VLP density of  $17.6 \times 10^9 \text{ particles/ml}$ .

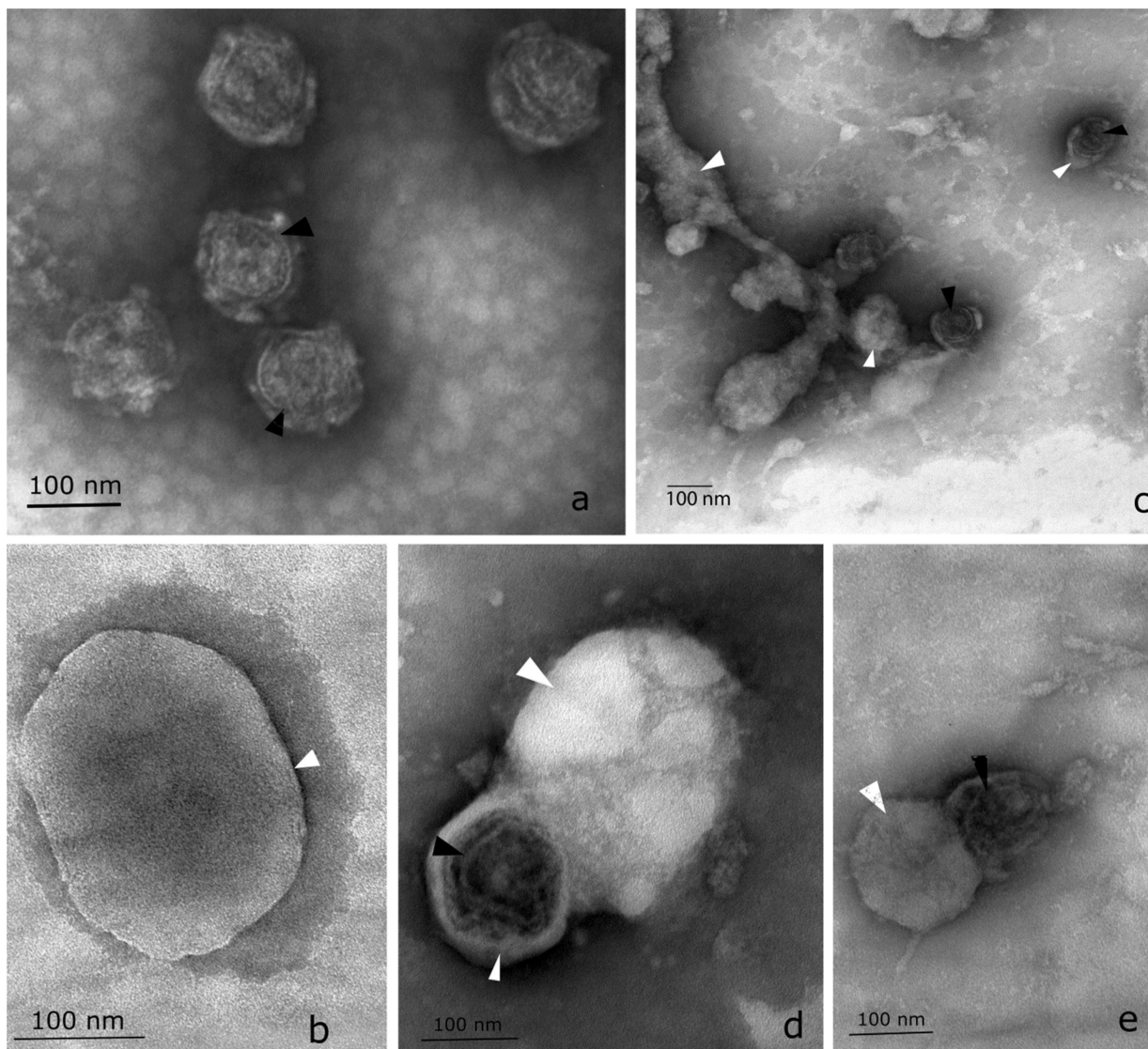


**Figure 2.** Uptake of  $\phi$ /M-VLP in HEK293 cells at (a)  $5 \mu\text{g}/10^9$  M-VLP, (b)  $10 \mu\text{g}/10^9$  M-VLP and (c)  $20 \mu\text{g}/10^9$  M-VLP. M-VLP were labeled with fluorescent lipophilic dye DiD prior to complexing with liposomes. Ten thousand cells were measured for each vector. Transfections were performed with  $1 \times 10^9$  M-VLP/well of a 12-well tissue culture plate with vector formation using M-VLP density of  $29.1 \times 10^9$  particles/ml.

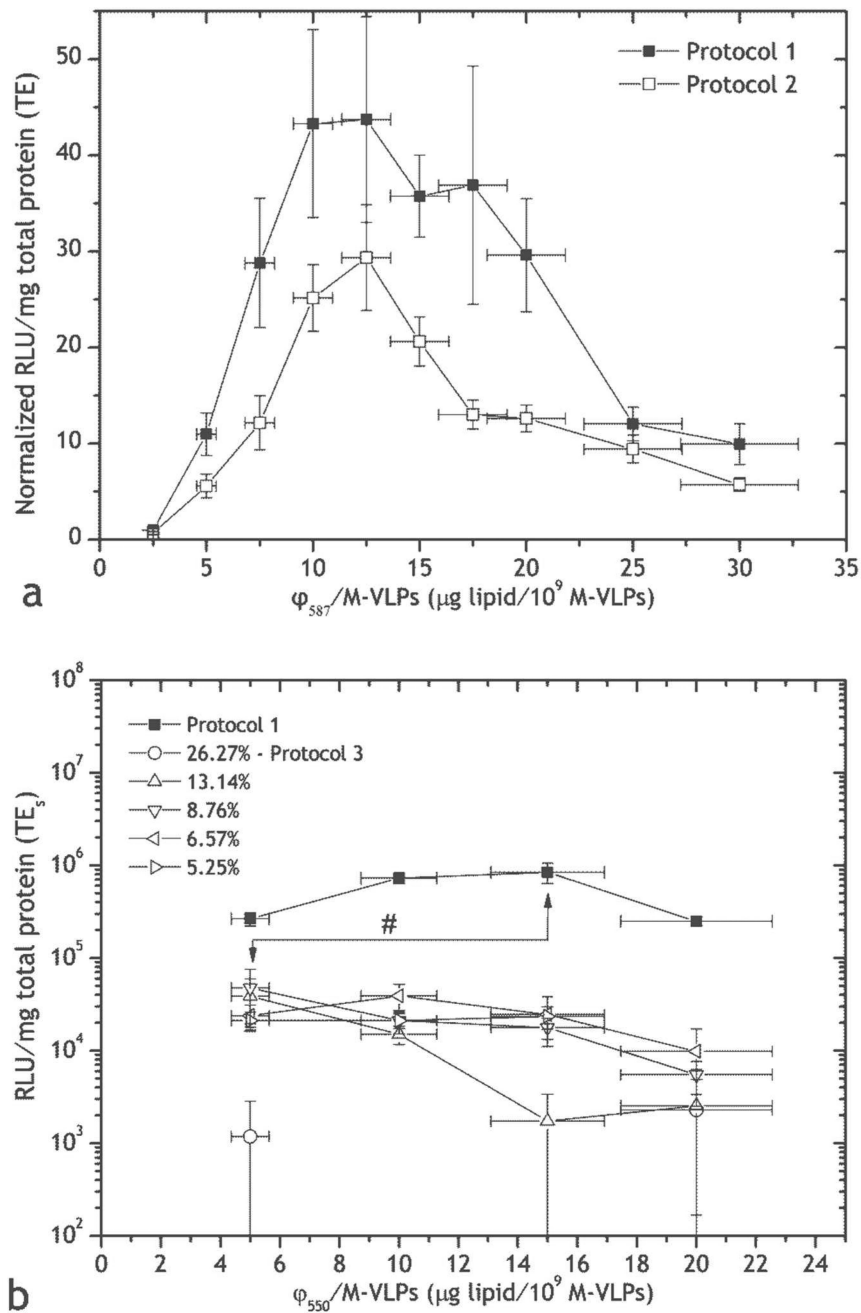


**Figure 3.** Cytotoxicity in HEK293 cells exposed to liposomes with compositions  $\phi_{587}$ ,  $\phi_{505}$  and  $\phi_{550}$ . Absorbance values of treated cells were normalized to untreated cells. Error bars indicate standard deviation (n=3).





**Figure 4.** Negative-stained transmission electron micrographs of (a) M-VLP alone (b)  $\phi_{587}$  extruded and  $\phi_{587}$ /M-VLP at  $5 \mu\text{g}/10^9$  M-VLP using (c) Protocol 1 (d) Protocol 2 and (e) Protocol 3. Solid black arrows indicate M-VLPs; solid white arrows indicate liposomes. Scale bar = 100 nm.

**Figure 5.**

Transgene expression in HEK293 cells transfected with  $\phi_{587}$ /M-VLP at  $1 \times 10^9$  M-VLP/well of a 12-well tissue culture plate formed via (a) Protocol 2 and (b) Protocol 3. (a) RLU/mg total protein = Relative light units per mg of total protein in cellular lysate normalized to the same measurement at a lipid stoichiometry of  $2.5 \mu\text{g}/10^9$  M-VLP of  $\phi_{587}$ /M-VLP formed via Protocol 1. Error bars indicate standard deviation. (b) RLU/mg total protein = Relative light units per mg of total protein in cellular lysate. The hybrid vectors were formed with different concentrations of ethanol as a percentage of the M-VLP containing DMEM supernatant from 5.25% to 26.27%. # -  $p < 0.005$ .

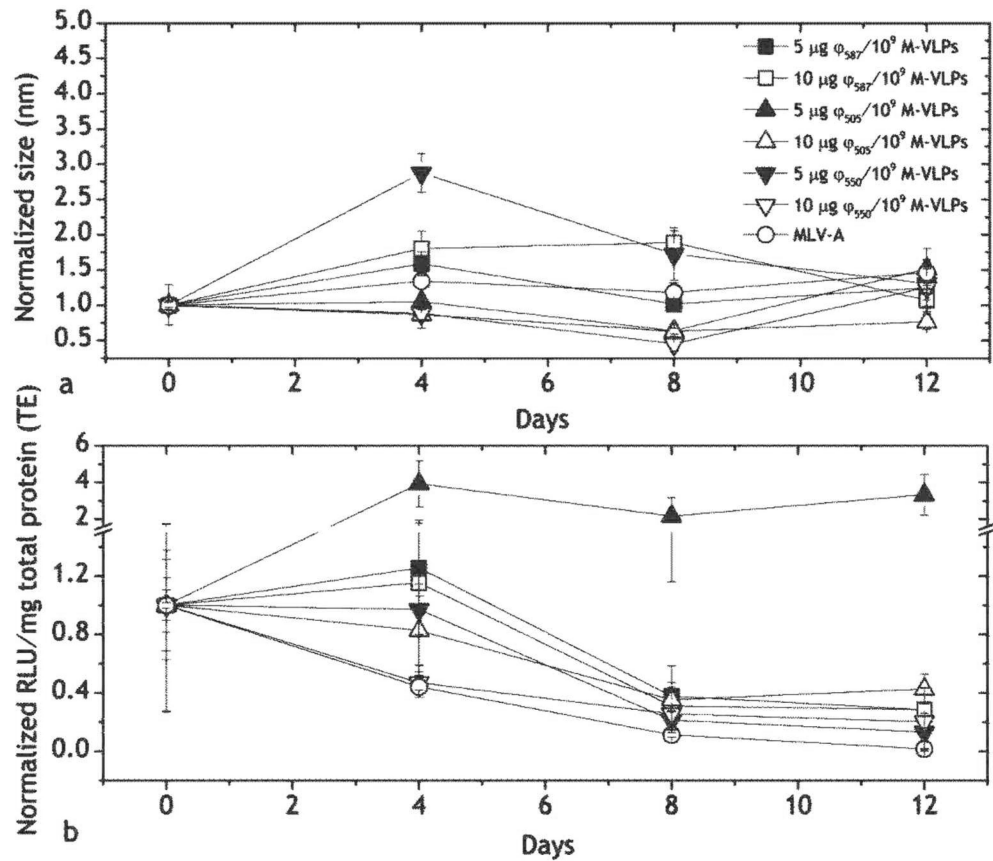


**Figure 6.**

Storage stability of  $\phi_{587}$ /M-VLP,  $\phi_{505}$ /M-VLP and  $\phi_{550}$ /M-VLP at  $10 \mu\text{g}/10^9$  M-VLP in comparison to MLV-A in terms of (a) size and (b) transfection efficiency over 12 days. (a) Size in nm of all vectors normalized to size on day 0. (b) Normalized RLU/mg total protein = relative light units per mg total protein in cellular lysate normalized to the same expression on day 0 for each vector.

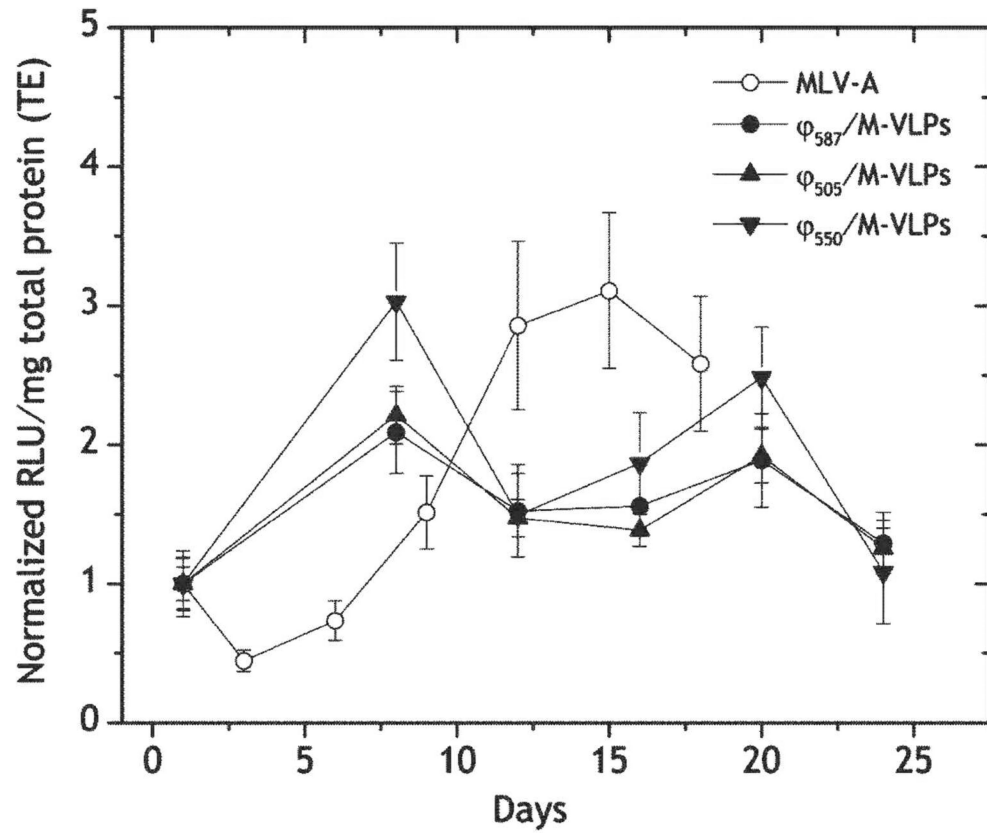


**Figure 7.** Stability of transgene expression in HEK293 cells transfected with  $\phi_{587}$ /M-VLP,  $\phi_{505}$ /M-VLP,  $\phi_{550}$ /M-VLP at  $5 \mu\text{g}/10^9$  M-VLP and MLV-A over three weeks. Normalized RLU/mg total protein = relative light units per mg total protein in cellular lysate normalized to the same expression on day 1. Error bars indicate standard deviation (n=3).

Table 1

Sizes (in nm) measured via Dynamic Light Scattering of  $\phi 587/M-VLP$ ,  $\phi 505/M-VLP$  and  $\phi 550/M-VLP$ . The size of M-VLP without addition of any lipid was  $93 \pm 4$  nm. Mean  $\pm$  SEM (n=2).

Protocols	Type	Lipid only	Size (nm)		
			Lipid/M-VLP ratios ( $\mu\text{g}/10^9$ M-VLP)	5	10
Dry Film Method (1)	$\phi 587/M-VLP$	269 $\pm$ 8	278 $\pm$ 10	697 $\pm$ 60	1916 $\pm$ 99
	$\phi 505/M-VLP$	353 $\pm$ 5	443 $\pm$ 6	601 $\pm$ 7	758 $\pm$ 12
	$\phi 550/M-VLP$	294 $\pm$ 48	493 $\pm$ 114	1190 $\pm$ 184	1754 $\pm$ 60
Lipid Extrusion (2)	$\phi 587/M-VLP$	176 $\pm$ 3	334 $\pm$ 5	374 $\pm$ 10	329 $\pm$ 7
	$\phi 505/M-VLP$	172 $\pm$ 3	235 $\pm$ 5	244 $\pm$ 5	483 $\pm$ 12
	$\phi 550/M-VLP$	134 $\pm$ 2	202 $\pm$ 2	397 $\pm$ 8	1759 $\pm$ 99
Alcohol Injection (3)	$\phi 550/M-VLP$	183 $\pm$ 1	320 $\pm$ 7	271 $\pm$ 4	305 $\pm$ 3